IEEE Access
Multidisciplinary | Rapid Review | Open Access Journal

Received November 15, 2019, accepted December 3, 2019, date of publication December 12, 2019,
date of current version December 23, 2019.

Digital Object Identifier 10.1109/ACCESS.2019.2959009

Carrier Phase Recovery for Array Navigation Receiver : A Fast Phase Retrieval Approach

QIANG LI[1], LEI HUANG[1], (Senior Member, IEEE), WEI LIU[2], (Senior Member, IEEE), BO ZHAO[1], (Member, IEEE), AND PEICHANG ZHANG[1]

[1]Guangdong Laboratory of Artificial Intelligence and Digital Economy (SZ), College of Electronic and Information Engineering, Shenzhen University, Shenzhen 518060, China
[2]Department of Electronic and Electrical Engineering, University of Sheffield, Sheffield S10 2TN, U.K.

Corresponding author: Lei Huang (lhuang@szu.edu.cn)

This work was supported in part by the National Natural Science Foundation of China under Grant 61801302, Grant 61925108, Grant U1713217, Grant U1913203, Grant 61801297, and Grant 61601304.

ABSTRACT A fast carrier phase recovery scheme is developed for satellite navigation receiver using an antenna array based on the phase retrieval theory, in which the antenna array provides sufficient measurement information for the phase recovery algorithm. First, the complex satellite signal model after coherent integration is established using the antenna array. Then, considering symbol uncertainty of the navigation data during the coherent integration time, the carrier phase estimation is formulated as a typical phase retrieval problem. At last, using the squared iterative method (SQUAREM), which is capable of superlinear convergence, a fast variant of the Wirtinger Flow (WF) algorithm is derived to solve the phase recovery problem efficiently without compromising the balance between simplicity and stability. As demonstrated by numerical results, the proposed algorithm outperforms the state-of-the-art in terms of the mean squared error (MSE) convergence. Moreover, the adjustment processes of the carrier phase in the proposed method is validated.

INDEX TERMS Phase retrieval, antenna array, carrier phase recovery, Wirtinger Flow, superlinear convergence.

I. INTRODUCTION

Recently, research on high-precision positioning using satellite navigation receiver, such as the global positioning system (GPS), has attracted significant attention in the military and safety-critical fields [1]–[3]. Normally, high-precision positioning is achieved by estimating the carrier phase of satellite signals in phase-locked loop (PLL). However, the PLL is very vulnerable to radio frequency (RF) interferences [3]. Therefore, the carrier phase recovery problem in the presence of interferences poses a big challenge in satellite navigation receiver [4].

In a GPS receiver, the effective signal-to-noise ratio (SNR) is reduced by interferences, which is equivalent to an attenuation of the received GPS signal itself [5]. In order to enhance the tracking capability of the GPS receiver in such an environment, various approaches have been proposed. In broad terms, these approaches include designing an adaptive loop filter [6], improving loop architecture [5], multi-sensor fusion [2], beamforming based on antenna array [7]–[9], and so on. The work in this paper will be focused on the antenna array technique given its excellent spatial interference suppression capability, and the extra diversity provided for phase retrieval compared with schemes based on a single antenna.

In recent years, a new class of phase recovery algorithms are widely used in the fields of image and audio signal processing [10], [11]. In the absence of phase information, the original image or signal can still be reconstructed with high probability when the number of measurements is large enough, which is normally four times the dimension of the original signal [12]. Using the alternating minimization technique [13], the Gerchberg-Saxton (GS) algorithm was developed to solve the phase retrieval problem [14]. Another popular method is based on the semidefinite programming (SDP) technique and the rank-1 matrix recovery framework [10]. However, the ''matrix-lifting'' problem will occur in the case of high dimensional incident signals [15]. More recently, using the steepest descent method with a heuristic step, a Wirtinger Flow (WF) algorithm was proposed to solve the phase retrieval problem [16]. Moreover, associated

The associate editor coordinating the review of this manuscript and approving it for publication was Giorgio Montisci.

This work is licensed under a Creative Commons Attribution 4.0 License. For more information, see http://creativecommons.org/licenses/by/4.0/

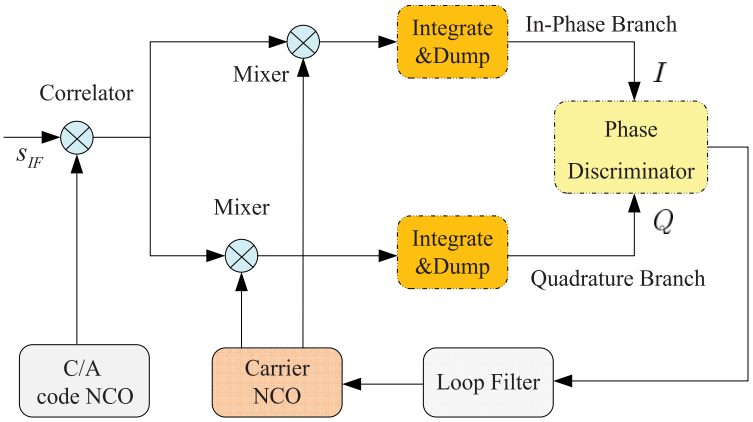

FIGURE 1. Block diagram of of a standard PLL.

with the majorization-minimization (MM) framework, three new phase retrieval algorithms, called PRIME-Single-Term, PRIME-Both-Terms and PRIME-Power, were proposed in [17], where the phase retrieval problem is solved using a surrogate optimization approach with a simple closed-form solution at each iteration. However, due to multiple parameters majorization or high-dimensional eigen-decomposition, the PRIME-Both-Terms and PRIME-Power algorithms have potentially a slower convergence rate. Besides, a truncated amplitude flow (TAF) algorithm was presented in [18] by employing the magnitudebased least squares cost function. Furthermore, for the phase retrieval of sparse signals, a sparse TAF algorithm with a recovery guarantee was developed in [19]. More recently, associating compressive phase retrieval via majorization-minimization technique (C-PRIME) with the convex ℓ_1-norm penalty term, a phase retrieval approach encouraging sparse solution was proposed in [20], where the phase retrieval problem is formulated into the least-absolute-shrinkage-and-selection-operator (LASSO) form. However, its convergence rate is usually slow.

In this paper, we consider the carrier phase recovery problem from the perspective of phase retrieval theory, which is different from the view of traditional PLL. Due to the symbol uncertainty of navigation data during the coherent integration period, the carrier phase estimation in GPS receiver is transformed into a phase retrieval problem by employing an antenna array. As well known, the antenna array not only has the interference suppression capability in the spatial domain, but also can capture more spatial measurement information. In this work, the antenna array will acquire sufficient number of measurements for the phase retrieval algorithm to recover the carrier phase with a high probability. Furthermore, on the basis of the WF algorithm, the squared iterative method (SQUAREM) in [21] is modified to handle the phase retrieval problem, ending up with a new variant of SQUAREM with a faster convergence rate. To demonstrate the effectiveness of the proposed approach, the mean squared error (MSE) performance of carrier phase recovery are tested. Moreover, the adjustment processes of the carrier phase in the proposed method and traditional PLL are compared.

Furthermore, we also investigated other popular accelerator methods published in recent years. Over-relaxation acceleration is proposed in [22], in which computing the optimal parameter α is generally a difficult problem. In [23], a fast iterative shrinkage-thresholding algorithm is proposed to solve linear inverse problem. More recently, one accelerator method via backtracking is proposed in [24]. But it is not easy to guarantee convergence accuracy because a loose approximation of the original objective function should be used.

II. PROBLEM FORMULATION

In the signal tracking process, the baseband receiver tracks the coarse-acquisition (C/A) code phase, carrier frequency and carrier phase of the received satellite signal. Specifically, the C/A code phase tracking is performed using delay-locked loop (DLL), whereas the carrier tracking is accomplished by PLL, frequency-locked loop (FLL) or the combination of PLL and FLL [5]. In the tracking loops mentioned above, the PLL has been widely used in the high-precision positioning field because its output measurement value of the carrier phase is quite accurate in many cases.

A block diagram of a typical PLL structure is shown in Fig. 1. It consists of a pair of mixers, a carrier phase discriminator, a loop filter and a numerically controlled oscillator (NCO). In the PLL, the phase discriminator is used to estimate the carrier phase error from the In-Phase/Quadrature (I/Q) branches. Then, the output of the phase discriminator goes through a loop filter to generate a signal which drives the NCO. Subsequently, the NCO generates a replica signal whose phase is synchronized to that of the incoming signal [25].

In the tracking loop of the traditional satellite navigation receiver with a single antenna, the coherent integration values of the prompt I/Q branches after the integrate and dump processes [25] are respectively expressed as

$$I(t) = \sqrt{p}D(t)R\left(\zeta(t)\right)\operatorname{sinc}\left(\Delta f(t)T_{coh}\right)\cos\Delta\phi(t) \quad (1)$$

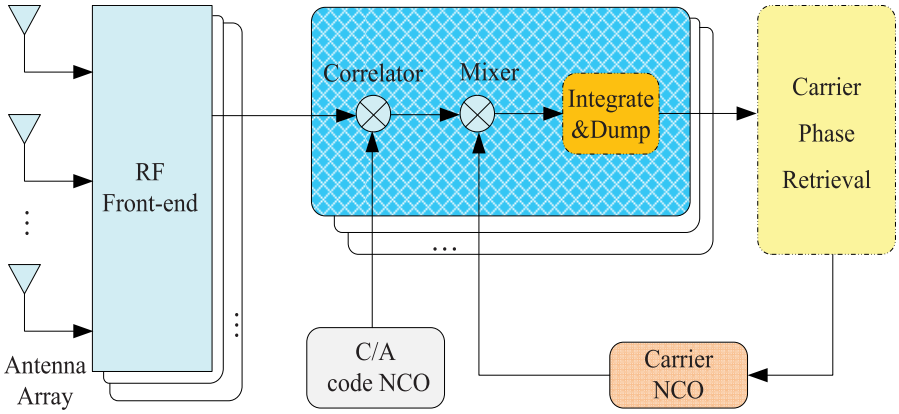

FIGURE 2. Block diagram of carrier phase retrieval with antenna array.

$$Q(t) = \sqrt{p}D(t)R\left(\zeta(t)\right)\operatorname{sinc}\left(\Delta f(t)T_{coh}\right)\sin\Delta\phi(t) \quad (2)$$

where t represents the sampling time, p is the signal power, D stands for the bit stream of the navigation data with uncertain symbol ± 1, ζ is the C/A code phase delay, $R(\cdot)$ stands for the auto-correlation function (ACF) of the C/A code, T_{coh} is the coherent integration time, Δf and $\Delta\phi$ represent the frequency error and the phase error between the received signal and the locally generated replica, respectively.

Then, the phase error $\Delta\phi$ can be calculated using the phase discriminator in the PLL

$$\Delta\phi(t) = \arctan\{Q(t)/I(t)\} \quad (3)$$

where, arctan is the inverse tangent function.

It should be noted that the traditional PLL is simple, but its tracking ability is very weak and it is easy to lose the lock in the presence of interferences. It is widely known that the navigation receiver with an antenna array can effectively suppress interferences in the spatial domain, which has been widely studied in the literature [26]. In the following sections, we will exploit another advantage of the antenna array considering that it can provide more spatial measurement information, based on which a new carrier phase estimation scheme from the framework of phase retrieval theory is then proposed.

III. PROPOSED CARRIER PHASE ESTIMATION VIA PHASE RETRIEVAL

In this section, we will first design the scheme of carrier phase retrieval for a GPS receiver equipped with antenna array and transform the carrier phase estimation problem into a new phase recovery problem. After that, we extend the scheme of SQUAREM to the WF algorithm and then develop a new phase retrieval algorithm with a fast convergence speed.

A. PHASE RETRIEVAL MODEL FOR GPS NAVIGATION

Fig. 2 shows the block diagram of carrier phase retrieval for a GPS receiver with an antenna array. First, the signals from GPS satellites are converted to the digital intermediate frequency (IF) after RF front-ends of the antenna array. Then, the IF signals enter into the baseband signal processing process, i.e., acquisition and tracking. Acquisition is the process of coarsely estimating the C/A code phase and carrier frequency of the visible satellite signals. After successful acquisition, the signal tracking process begins to work, which provides accurate estimates of the C/A code and carrier as they change over time. Different from the traditional PLL, the phase discriminator is replaced by the carrier phase retrieval module in Fig. 2. Moreover, the antenna array is used to provide spatial measurement information to the carrier phase retrieval module. In the following, the model derivation for carrier phase retrieval is provided in detail.

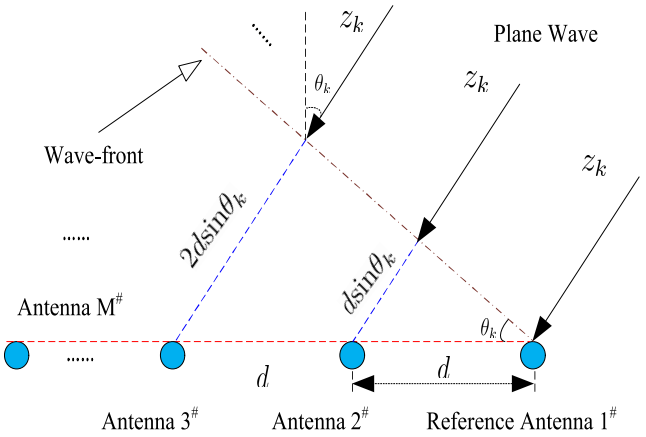

FIGURE 3. Diagram of incident signals at ULA antenna.

We consider a uniform linear array (ULA) consisting of M antennas and assume K satellite signals are received by the ULA. Fig. 3 shows the diagram of incident signals at ULA antenna, where d denotes the inter-element spacing and GPS signal is considered as far-field and narrow-band signal. First, we assume that direction of arrival (DOA) of the k-th signal at array antenna is θ_k and the k-th signal arriving at the reference antenna element can be expressed as

$$z_k(t) = \sqrt{2p_k}D_k(t)C_k(t)\sin(2\pi f_0 t) \quad (4)$$

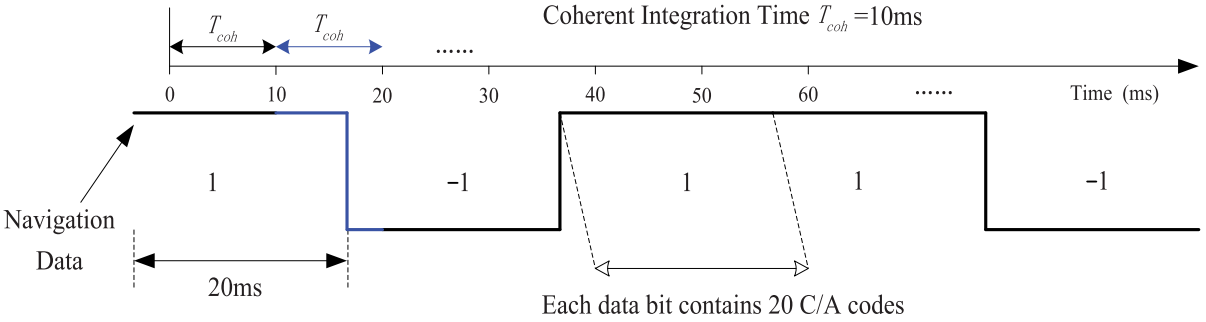

FIGURE 4. Diagram of navigation data and the coherent integration time.

where f_0 is signal frequency and C is spreading C/A code sequence. It should be noted that the C/A codes among different satellite signals are different and almost orthogonal which can reduce the mutual interference and is helpful for signal detection [27].

Then, for the k-th antenna element, the received signal is $z_k(t+\tau_m)$, where

$$\tau_m = \frac{(m-1)d\sin\theta_k}{c} \tag{5}$$

is time delay of the signal arriving at the m-th element compared with the reference element and c is the speed of light. According to the assumption that the GPS signal is narrowband [28], then we have

$$\begin{aligned} z_k(t+\tau_m) &\approx z_k(t)e^{j2\pi f_0\tau_m} \\ &= z_k(t)e^{j2\pi\frac{(m-1)d\sin\theta_k}{\lambda}} \end{aligned} \tag{6}$$

where λ is carrier wavelength of GPS signal. Therefore, all the incident signals at antenna array can be written as in (7) at the top of the next page.

$$\begin{bmatrix} u_1(t) \\ u_2(t) \\ \vdots \\ u_M(t) \end{bmatrix} = \begin{bmatrix} 1 & 1 & \cdots & 1 \\ e^{2\pi\frac{d\sin\theta_1}{\lambda}} & e^{2\pi\frac{d\sin\theta_2}{\lambda}} & \cdots & e^{2\pi\frac{d\sin\theta_K}{\lambda}} \\ \vdots & \vdots & \ddots & \vdots \\ e^{2\pi\frac{(M-1)d\sin\theta_1}{\lambda}} & e^{2\pi\frac{(M-1)d\sin\theta_2}{\lambda}} & \cdots & e^{2\pi\frac{(M-1)d\sin\theta_K}{\lambda}} \end{bmatrix} \times \begin{bmatrix} z_1(t) \\ z_2(t) \\ \vdots \\ z_K(t) \end{bmatrix} \tag{7}$$

In (7), $u_m(t)$ stands for all signals received by the m-th antenna element and we denotes steering vector as

$$\boldsymbol{a}(\theta_k) = \left[1, e^{j2\pi\frac{d\sin\theta_k}{\lambda}} \cdots e^{j2\pi(M-1)\frac{d\sin\theta_k}{\lambda}}\right]^T \tag{8}$$

Then, after the processes of integrate and dump [25], the signals of prompt I/Q branches, for the reference antenna element, are respectively expressed in the equations (1) and (2). Then, for the k-th signal, the complex signal is

$$\begin{aligned} x_k(t) &= I_k(t) + jQ_k(t) \\ &= \sqrt{p_k}D_k(t)R\left(\zeta_k(t)\right)\mathrm{sinc}\left(\Delta f_k(t)T_{coh}\right)e^{j\Delta\phi_k(t)} \\ &= b_k(t)e^{j\Delta\phi_k(t)} \end{aligned} \tag{9}$$

where $b_k(t) = \sqrt{p_k}D_k(t)R\left(\zeta_k(t)\right)\mathrm{sinc}\left(\Delta f_k(t)T_{coh}\right)$ and $\phi_k(t)$ are considered as the amplitude and phase of signal $x_k(t)$, respectively.

Similarly, for the whole antenna array, all the incident signals after the processes of integrate and dump can be expressed as

$$\boldsymbol{s}(t) = \boldsymbol{A}\boldsymbol{x}(t) \tag{10}$$

where $\boldsymbol{s} = [s_1, s_2 \cdots s_M]^T$, s_m stands for all signals received by the m-th antenna element, $\boldsymbol{A} = [\boldsymbol{a}(\theta_1), \boldsymbol{a}(\theta_2) \cdots \boldsymbol{a}(\theta_K)]$, $\boldsymbol{x} = [x_1, x_2 \cdots x_K]^T$ and t is omitted for notational simplicity in the following.

It should be noted that after the acquisition process of the satellite navigation receiver, the ranges of both the C/A code phase delay ζ and the frequency error Δf can be determined in (9). Specifically, $\zeta \in (-0.5, 0.5)$ stands for the chip of the C/A code and Δf is actually the Doppler frequency from the satellite to the antenna array, satisfying $\Delta f \in (-10, 10)$ kHz.

But for the navigation data D, its value may change during the coherent integration time T_{coh}. Specifically, for GPS signal, the period of C/A code and navigation data code are 1ms and 20ms, respectively [27]. The coherent integration time should be an integral multiple of 1ms and it is also less than or equal to 20ms. Generally, the coherent integration time is set to 10ms. Fig. 4 shows a diagram of navigation data and the coherent integration time. It is observed that the navigation data values 1 and -1 are randomly distributed [30]. The starting moment of the coherent integration time is not aligned with the boundary of a navigation data bit. Therefore, the value of navigation data D may change during some coherent integration times [27]. For example, in the Fig. 4, the navigation data D (blue line) is changed in the second coherent integration time.

Therefore, in order to solve the problem, the paper formulates the carrier phase estimation in GPS receiver from the

viewpoint of phase retrieval scheme. Specifically, we consider the intensity measurement and reformulate (10) as

$$\boldsymbol{y} = |\boldsymbol{A}\boldsymbol{x}|^2 + \boldsymbol{n} \tag{11}$$

where $\boldsymbol{y}$ is the $M \times 1$ intensity measurement vector, $\boldsymbol{n} \in \mathbb{R}^M$ is the real-valued white Gaussian noise and $|\cdot|$ denotes the element-wise magnitude. Note that (11) is the standard model for phase retrieval. The task in this work is to recover the carrier phase signal $\boldsymbol{x}$.

B. PHASE RETRIEVAL VIA THE WF-SQUAREM ALGORITHM

According to the above derivation, the carrier phase estimation problem is formulated as recovering the K-dimensional complex signal $\boldsymbol{x}$ from the intensity of M linear measurements, which is a typical phase retrieval problem. Normally, to find a suitable solution, a general choice is to consider the following least squares problem

$$\min_{\boldsymbol{x}} \quad f(\boldsymbol{x}) = \left\| \boldsymbol{y} - |\boldsymbol{A}\boldsymbol{x}|^2 \right\|_2^2 \tag{12}$$

where $\|\cdot\|_2$ denotes the Frobenius norm. Notice that the optimization problem (12) is inherently non-convex and it is difficult to get a closed-form solution. Recently, employing the gradient descent technique, an efficient WF algorithm was proposed in [16] to solve the problem. The iterative procedure of the WF algorithm, for $t = 0, 1, 2, \cdots$, is

$$\boldsymbol{x}_{t+1} = \boldsymbol{x}_t - \frac{\mu_{t+1}}{\|\boldsymbol{x}_0\|_2^2} \nabla f\left(\boldsymbol{x}_t\right) \tag{13}$$

where $\boldsymbol{x}_0$ is an initial guess value, μ denotes an appropriate step size and $\nabla f(\boldsymbol{x}_t)$ denotes the gradient of the function $f(\boldsymbol{x})$ at the t-th iteration, which can be expressed as

$$\nabla f(\boldsymbol{x}_t) = 4\boldsymbol{A}^H \mathrm{diag}(|\boldsymbol{A}\boldsymbol{x}_t|^2 - \boldsymbol{y})\boldsymbol{A}\boldsymbol{x}_t \tag{14}$$

where $(\cdot)^H$ is conjugate transpose and $\mathrm{diag}(\cdot)$ is the operation of forming a diagonal matrix.

However, the WF method has the disadvantage that its convergence rate is slow. In order to further accelerate the convergence rate, we extend the SQUAREM scheme [21] to the WF method and propose a new WF-SQUAREM algorithm. Normally, the SQUAREM scheme can achieve a superlinear convergence rate with global convergence. The recursive relationship and convergence of the SQUAREM scheme have been proved in [21]. Instead of updating $\boldsymbol{x}_{t+1}$ directly from $\boldsymbol{x}_t$ at the t-th iteration, the SQUAREM scheme first introduces an intermediate point $\boldsymbol{\eta}$ based on $\boldsymbol{x}_t$ and then updates the next point $\boldsymbol{x}_{t+1}$ from the intermediate point. The proposed WF-SQUAREM algorithm is tabulated as follows.

It should be pointed out that in order to prevent the updating rule of the SQUAREM scheme from violating the descent property of the WF framework, a process of judgment and adjustment, i.e., the while loop, is inserted into the proposed algorithm. A simple variant of the back-tracking strategy is designed to repeatedly halve the distance between α and -1, i.e., $\alpha = (\alpha - 1)/2$ until $\|\boldsymbol{y} - |\boldsymbol{A}\boldsymbol{\eta}|^2\|_2^2 \leq \|\boldsymbol{y} - |\boldsymbol{A}\boldsymbol{z}_2|^2\|_2^2$. Even in the worst case where $\alpha = -1$, the intermediate point $\boldsymbol{\eta}$ satisfies $\boldsymbol{\eta} = \boldsymbol{x}_t + 2\boldsymbol{r} + \boldsymbol{u} = \boldsymbol{z}_2$, which ensures that the while loop can be terminated.

Algorithm 1 WF-SQUAREM Algorithm

Input: $\boldsymbol{A}, \boldsymbol{y}, M, K, \epsilon, \mu_{\max}, T$ (maximum iteration number)

Step 1. Initialize $\boldsymbol{x}_0$ as follows:

Set constant $\lambda^2 \leftarrow K \sum_{i=1}^{M} y_i \Big/ \|\boldsymbol{A}\|_2^2$,

$\boldsymbol{v} \leftarrow$ leading eigenvector of $\boldsymbol{A}^H \mathrm{diag}(\boldsymbol{y})\boldsymbol{A}$,

$\boldsymbol{x}_0 \leftarrow \lambda \boldsymbol{v}$.

for $t = 0, \cdots, T$ **do**

Step 2. $z_1 = \boldsymbol{x}_t - \frac{\mu_{t+1}}{\|\boldsymbol{x}_0\|_2^2} \nabla f\left(\boldsymbol{x}_t\right)$

where $\mu_{t+1} = \min(1 - e^{-(t+1)/\epsilon}, \mu_{\max})$

Step 3. $z_2 = z_1 - \frac{\mu_{t+1}}{\|\boldsymbol{x}_0\|_2^2} \nabla f\left(z_1\right)$

Step 4. $\boldsymbol{r} = z_1 - \boldsymbol{x}_t$

Step 5. $\boldsymbol{u} = z_2 - z_1 - \boldsymbol{r}$

Step 6. $\alpha = -\|\boldsymbol{r}\|_2 / \|\boldsymbol{u}\|_2$

Step 7. $\boldsymbol{\eta} = \boldsymbol{x}_t - 2\alpha\boldsymbol{r} + \alpha^2\boldsymbol{u}$

Step 8. **while** $\left\|\boldsymbol{y} - |\boldsymbol{A}\boldsymbol{\eta}|^2\right\|_2^2 > \left\|\boldsymbol{y} - |\boldsymbol{A}\boldsymbol{z}_2|^2\right\|_2^2$ **do**

$\alpha = (\alpha - 1)/2$

$\boldsymbol{\eta} = \boldsymbol{x}_t - 2\alpha\boldsymbol{r} + \alpha^2\boldsymbol{u}$

end while

Step 9. $\boldsymbol{x}_{t+1} = \boldsymbol{\eta} - \frac{\mu_{t+1}}{\|\boldsymbol{x}_0\|_2^2} \nabla f\left(\boldsymbol{\eta}\right)$

end for

Output: $\boldsymbol{x}_T$.

As mentioned in [17], due to the loss of phase information, the recovered signal may have an unknown constant phase shift with respect to the original signal $\boldsymbol{x}$. Therefore, an accurate phase shift needs to be calculated in the following procedure. After getting a solution $\boldsymbol{x}^*$ from the proposed algorithm, we define a function of MSE as

$$h(\psi) = \|\boldsymbol{x} - \boldsymbol{x}^* \cdot e^{j\psi}\|_2^2, \tag{15}$$

where ψ denotes the constant phase shift. The derivative of $h(\psi)$ with respect to ψ is

$$\nabla h(\psi) = j[(\boldsymbol{x}^*)^H \boldsymbol{x} \cdot e^{-j\psi} - \boldsymbol{x}^H \boldsymbol{x}^* \cdot e^{j\psi}]. \tag{16}$$

Setting the derivative equal to zero, we have

$$e^{j\psi} = \frac{(\boldsymbol{x}^*)^H \boldsymbol{x}}{|(\boldsymbol{x}^*)^H \boldsymbol{x}|}. \tag{17}$$

Finally, $\boldsymbol{x}^* \cdot e^{j\psi}$ gives the recovered signal.

IV. SIMULATION RESULTS

In the following experiments, we consider a ULA consisting of $M = 50$ antennas unless specified otherwise, where the inter-element spacing d is set to half wavelength of the GPS L1 signal. GPS L1 signal consists of carrier, C/A code and navigation data, where the carrier frequency, C/A code frequency and navigation data frequency are 1575.42 MHz, 1.023 MHz and 50Hz, respectively. The carrier wavelength of GPS L1 signal is about 19 cm. The C/A codes belong

TABLE 1. Simulation parameters.

Parameter	Value	Parameter	Value
Baseband frequency	1.5 MHz	Sampling frequency	5 MHz
C/A code loop bandwidth	25 MHz	C/A code loop gain	1 Hz
Carrier loop bandwidth	16 MHz	Carrier loop gain	0.25 Hz
Damping coefficient	0.707	Correlator spacing	0.5 chip

to the family of Gold codes, which are generated from the product of two 1023-bit pseudorandom noise (PRN) sequence [27]. Navigation data is a bit stream of the navigation data with uncertain symbol ± 1. The additive noise is modeled as an independent Gaussian process with zero mean and unit variance. The number of GPS signals is $K = 10$ and the DOAs of the 10 GPS signals are set to $-65^\circ, -45^\circ, -30^\circ, -20^\circ, -10^\circ, 0^\circ, 10^\circ, 30^\circ, 50^\circ$ and 70°, respectively.

Moreover, we also assume that the coherent integration time $T_{coh} = 10$ms, the code phase and Doppler frequency have been synchronized, which means that the C/A code phase delay $\zeta = 0$ and the frequency error $\Delta f = 0$. Therefore, $R(\zeta_k) = 1$ and $\text{sinc}(\Delta f_k T_{coh}) = 1$. Meanwhile, The SNRs of GPS signals are set to 20 dB after C/A code sequences are synchronized, which is reasonable and consistent with the actual application of GPS receiver [30].

The phase error $\Delta\phi_k, k = 1, \ldots, K$ is randomly distributed between 0 and 2π. Furthermore, for the proposed WF-SQUAREM algorithm, the heuristic step size μ in (13) is chosen as the same as that in [16], where the values of ε and $\mu_{\max}$ are initialized as 330 and 0.3, respectively. In the following experiments, 500 Monte-Carlo runs are performed. The main simulation parameters of the software-defined GPS receiver [31] are listed in Table 1 unless otherwise

A. COHERENT INTEGRATION ATTENUATION VERSUS FREQUENCY ERROR

In the equations (1-2) and (9), the frequency error Δf affects the results of coherent integration. The coherent integration of signal is beneficial to improve the SNR [30]. Fig. 5 shows the relationship of coherent integration attenuation $\text{sinc}(\Delta f T_{coh})$ versus frequency error Δf. It is observed that the function $\text{sinc}(\Delta f T_{coh})$ gets its maximum value 1 in the case of $\Delta f = 0$. Thus, there is no attenuation in the result of coherent integration, which is beneficial to improve the SNR of signal. Otherwise, if Δf is not equal to 0, the result of coherent integration will be partially attenuated, which will reduce the SNR of signal and make it difficult to detect and track signal to some extent [30]. Also, the similar case will happen if code phase is not synchronized, because the auto-correlation function $R(\cdot)$ could not get its maximum value 1.

B. RECOVERED MAGNITUDE AND PHASE COMPARISONS

Firstly, for the proposed WF-SQUAREM algorithm, in order to compare the magnitudes of the recovered signal and the original signal intuitively, the magnitude curves are shown in Fig. 6 at the 50th iteration. It is observed that, at the DOAs of the 10 GPS signals, the magnitudes in the recovered signal are almost the same as those in the original signal, which proves that the proposed WF-SQUAREM algorithm can recover the magnitude information of original signal successfully.

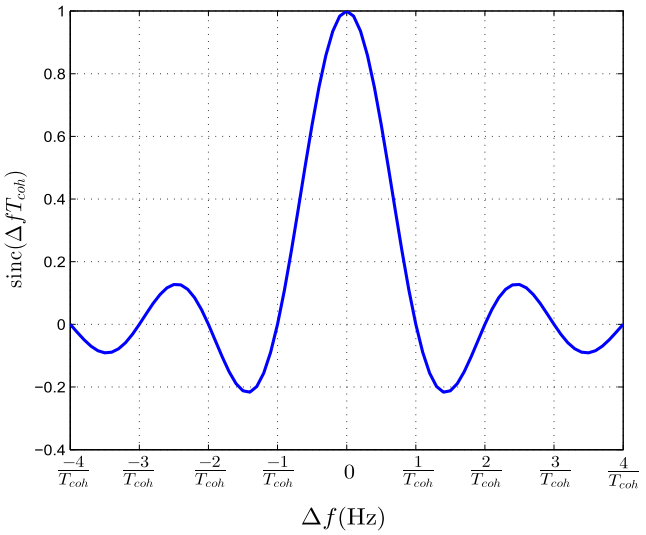

FIGURE 5. Coherent integration attenuation versus frequency error.

Furthermore, to verify the recovering ability of phase information, Fig. 7 plots the original signal and recovered signal when the number of iterations is 1, 10 and 50, respectively, where we can observe the iteration process of the proposed WF-SQUAREM algorithm. Specifically, it can be seen from the iterative process that the recovered signal is a random complex vector at the first iteration. As the number of iterations increases, the position of the recovered signal becomes close to that of the original signal. After 50 iterations, the phase of the recovered signal is almost the same as that of the original signal, showing an excellent phase recovery ability of the WF-SQUAREM algorithm.

C. MSE OF RECOVERD SIGNAL VERSUS THE NUMBERS OF ANTENNAS

Then, we test the MSE performance of the proposed WF-SQUAREM algorithm with different numbers of antennas. In this paper the number of antenna elements M affects steering vector $\boldsymbol{a}(\theta)$ in (8) and matrix $\boldsymbol{A}$ in (11), and then

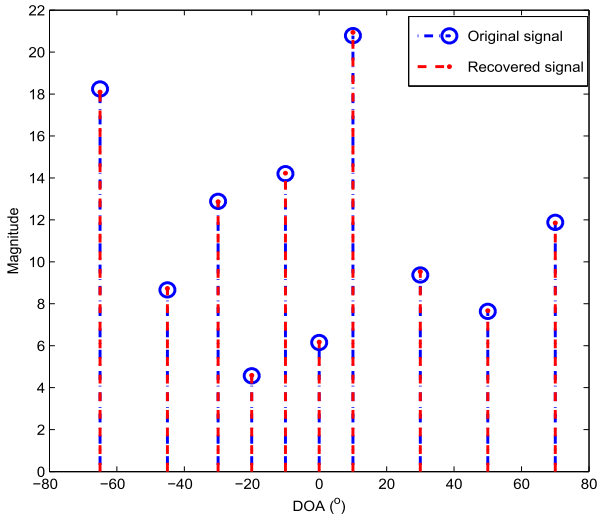

FIGURE 6. Original and recovered signals.

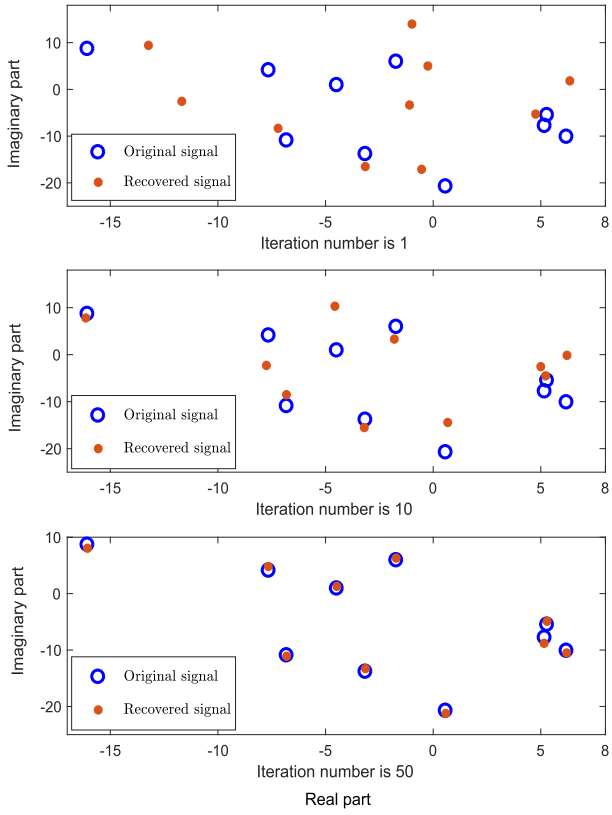

FIGURE 7. Original and recovered signals.

determines the gradient $\nabla f(\boldsymbol{x})$ in (14) which affects the convergence rate of the proposed method. Fig. 8 shows the MSE results versus the iteration number in the cases of $M = \{20, 25, 30, 40, 50\}$. It is observed that, for $M = 20$, i.e., the MSE value is stable at about 10 and does not change any more as the number of iterations increases. For the other cases, the MSE values decrease gradually with the increase of iterations. Moreover, Fig. 8 also depicts that the MSE curves

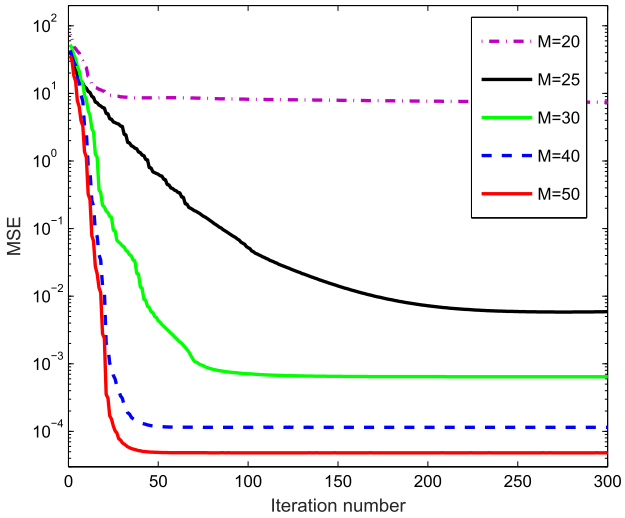

FIGURE 8. MSE of WF-SQUAREM algorithm versus iteration number, $M = \{20, 25, 30, 40, 50\}$.

have a much faster convergence rate and a much lower steady-state value as the number of antennas increases. After a large number of experiments, we find that the convergence rate of MSE curves starts to get faster when the number of antennas is more than twice the number of signals. Specifically, the values of MSE are significantly improved after $M = 20$, which is because more suitable gradients are obtained by using more measurement data.

Moreover, the MSE of $M = 20$ has the higher steady-state value of 7.5 and the steady-state values of $M = \{30, 40, 50\}$ are about 6×10^{-4}, 1×10^{-4} and 5×10^{-5}, respectively. Similar to [17], we also assume that an algorithm has successfully recovered the original signal if the MSE is less than or equal to 10^{-4}. Based on this criterion, only in the cases of $M = \{40, 50\}$, the WF-SQUAREM algorithm can successfully recover the original signal, which is consistent with the statement in [12] that about $4K$ measurements are required for a successful recovery.

D. MSE COMPARISON OF DIFFERENT ALGORITHMS

This paper considers the problem that the updating rule of the SQUAREM scheme [21] may violate the descent property of the WF framework and designs a process of judgment and adjustment, i.e., the while loop (Step 8) in the proposed algorithm, The Fig. 9 shows the MSE of WF-SQUAREM algorithm with and without Step 8. It is observed that the MSE curve without Step 8 has many obvious outliers and it could not approach the steady state like the case with Step 8.

Moreover, to compare the MSE performance of the proposed WF-SQUAREM algorithm with the existing WF [16], FISTA [23], GS [14], PRIME-Single-Term, PRIME-Both-Terms and PRIME-Power algorithms [17], the MSE curves of the above-mentioned algorithms are shown in Fig. 10. It should be noted that the original FISTA algorithm in [23] is used to tackle the general linear inverse problem with a fast convergence rate. In this paper, combining the model

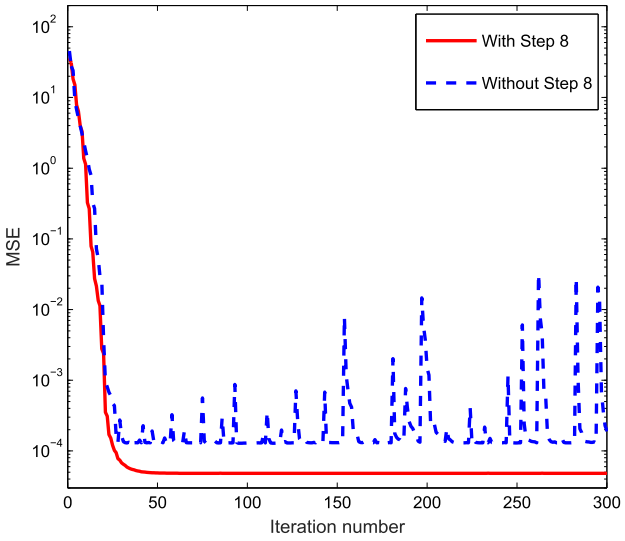

FIGURE 9. MSE of WF-SQUAREM algorithm with and without Step 8.

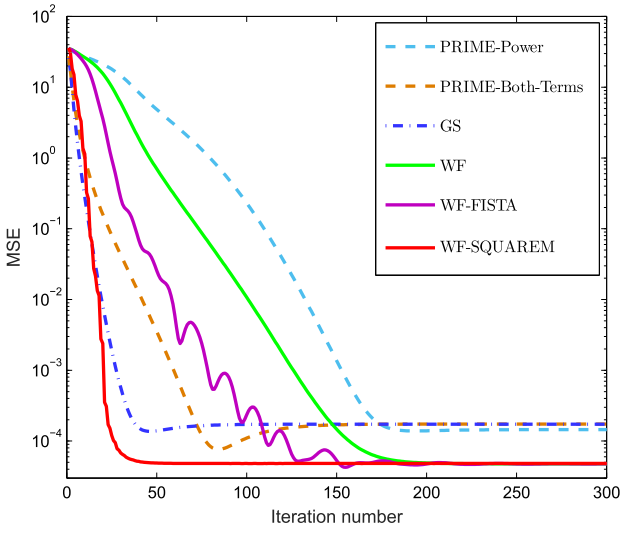

FIGURE 10. Comparison of MSE versus iteration number, $M = 50$.

of the WF algorithm, the FISTA technique can solve the phase retrieval problem, which is abbreviated as the WF-FISTA algorithm. Moreover, as mentioned in [17], the PRIME-Single-Term algorithm has the same solution as the GS algorithm but from a different majorization-minimization perspective. Therefore, the MSE curve of PRIME-Single-Term is not shown in Fig. 10.

As can be seen, all the MSE curves decrease rapidly and converge gradually with an increasing iteration number. Specifically, the GS, PRIME-Both-Terms and PRIME-Power algorithms have an approximate steady-state value close to 2×10^{-4} and the WF, WF-FISTA and WF-SQUAREM algorithms have the same steady-state value 5×10^{-5}, which is lower than that of the GS, PRIME-Both-Terms and PRIME-Power algorithms. However, the GS algorithm has a relatively faster convergence rate than the other methods except for the proposed WF-SQUAREM algorithm. Compared with the GS algorithm, the PRIME-Both-Terms algorithm has more parameters to be optimized which results in a slower convergence rate. For the PRIME-Power algorithm, the measurement matrix $\boldsymbol{A}$ is column vectorized and then a high dimensional intermediate matrix needs to be eigen-decomposed, which is computationally costly and time consuming.

On the other hand, although the WF and WF-FISTA algorithms have a lower steady-state value, their convergence rate is slower than the GS and PRIME-Both-Terms algorithms. Furthermore, the MSE values of the WF-FISTA algorithm are smaller than those of the WF algorithm before the number of iterations reaches 160, as the WF-FISTA algorithm has used more *a priori* information. Overall, the proposed WF-SQUAREM algorithm has a lower steady-state value than the GS method and also outperforms in terms of MSE convergence rate the other tested approaches because of the superlinear convergence ability of the SQUAREM method.

E. COMPARISON OF ADJUSTMENT PROCESS OF CARRIER PHASE ERROR

In order to compare the adjustment processes of the carrier phase in traditional PLL and the proposed method, the software-defined GPS receiver [31] is used where the simulation parameters in Table 1. Fig. 11 shows the carrier phase errors versus the update number of PLL. It is observed that the carrier phase errors of the 10 GPS signals have obvious oscillation during convergence process but decrease gradually with the increase of iterations. These phase errors have an approximate steady-state value about 0 when the update number of PLL reaches 110-120.

Fig. 12 depicts the carrier phase error versus iteration number of the proposed method, where the number of iterations is based on the proposed algorithm itself rather than on the PLL hardware. Compared with the PLL method, the phase error curves of the proposed algorithm do not have the oscillatory behaviour and converge directly to their steady-state values, close to 0 when the number of iterations reaches 23-25. Moreover, it can be seen from Figs. 11 and 12 that, although the adjustment processes of the carrier phase errors are different, the their steady-state values are nearly same, close to 0.

F. MULTIPATH EFFECTS ON CARRIER AND CODE PHASE

Multi-path may cause measurement errors of C/A code phase and carrier phase. For the code tracking loop, multi-path will distort the curve of autocorrelation function $R(\cdot)$ and then affect the measurement of the code phase to some extent [29]. Fig. 13 depicts the code phase measurement error versus muti-path dealy, where γ represents correlator spacing. It is seen that the muti-path can cause 0.25 chip (about 75 meters) code phase error in the case of $\gamma = 0.5$ chip and code phase error only has 0.05 chip (about 15 meters) when $\gamma = 0.1$. Therefore, correlator with narrow-spacing is a choice for multi-path suppression.

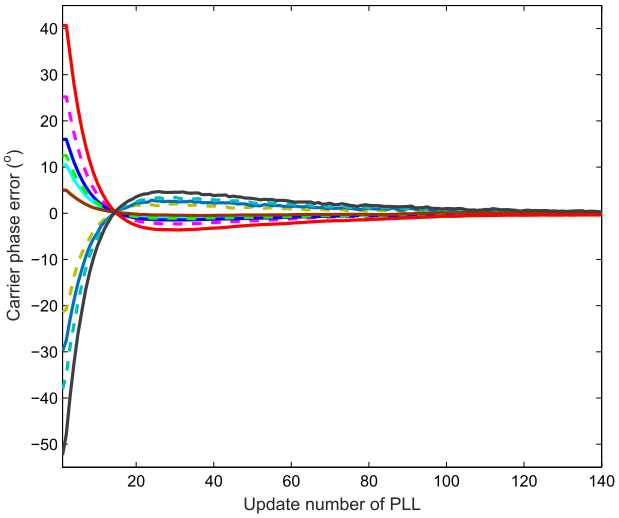

FIGURE 11. Phase error versus update number of PLL.

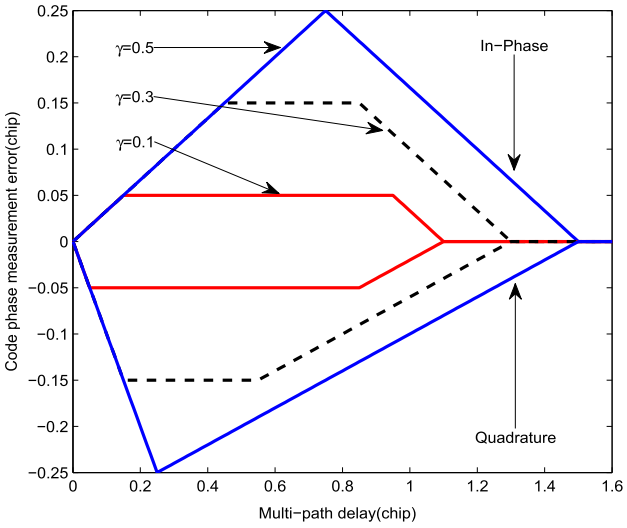

FIGURE 13. Code phase measurement error versus muti-path dealy.

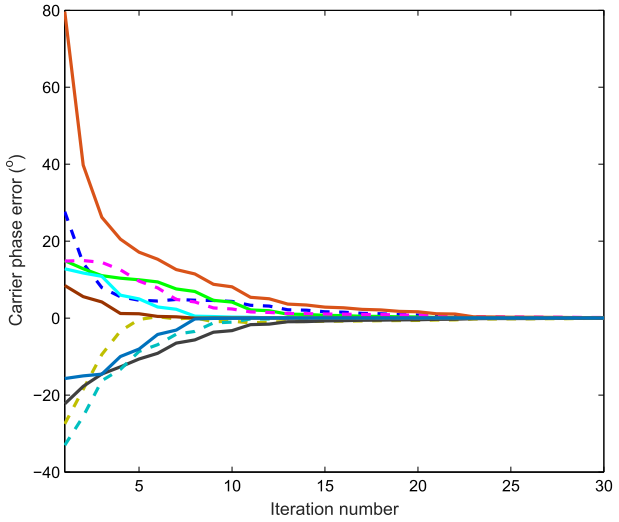

FIGURE 12. Phase error versus iteration number of the proposed method.

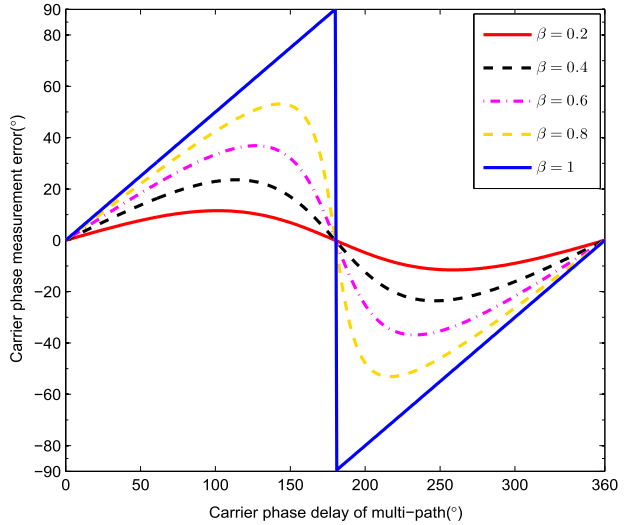

FIGURE 14. Carrier phase measurement error versus carrier phase delay of multi-path.

For the carrier tracking loop, Fig. 14 shows the carrier phase measurement error versus carrier phase delay of multi-path in the case of $\beta = [0.2, 0.4, 0.6, 0.8, 1]$, where β denotes amplitude ratio of multipath to direct signal, i.e., attenuation coefficient of multi-path. It is seen that carrier phase measurement error becomes smaller as the attenuation coefficient decreases. Specifically, when attenuation coefficient of multi-path $\beta = 1$, we get the maximum value of carrier phase measurement error $\pm 90°$, i.e., 0.25 carrier wavelength or 4.75cm, which is less than 1cm in general.

Stated thus, compared with C/A code tracking loop, multipath has little effect on carrier tracking loop. Moreover, if the carrier loop can track the direct signal well, multipath energy will be greatly attenuated after coherent integration and the multipath can be ignored in this case [30]. But if the code loop or carrier loop first locks the multipath signal, it will cause serious measurement error and tracking error. Then, multipath suppression must be considered in such a situation. This paper mainly considers the problem of symbol uncertainty of the navigation data during the coherent integration time and phase retrieval scheme. The fading and multi-path effects on our proposed method will be considered in future work.

V. CONCLUSION

In this work, different from the traditional PLL-based carrier phase estimation, the carrier phase of GPS signals has been recovered from the perspective of phase retrieval with the aid of an antenna array. Considering the symbol characteristic of complex satellite signals after coherent integration, the carrier phase estimation problem is transformed into a phase retrieval problem. Due to the loss of phase information, an antenna array is used to capture enough measurement information

to successfully recover the original signals. Moreover, a WF-SQUAREM algorithm has been proposed to solve the problem and the signal recovery process is also shown by numerical simulation results. Furthermore, the proposed method outperforms the existing methods in terms of the MSE convergence rate. At last, the adjustment process of the carrier phase error in the proposed method is compared with that in the traditional PLL method, where the effectiveness of carrier phase recovery of the proposed method has been validated.

Furthermore, the antenna array works in the case of passive sensing, i.e., all the antenna elements are used for ''receive only''. Therefore, some coprime arrays, such as the difference co-array of a co-prime pair which can work in passive sensing, also can be considered in this paper. The different is that the steering vector in (8) will change, which does not affect the proposed algorithm to get a suitable solution. In the future work, a detailed comparison of the ULA, coprime array and nested array will be done.

REFERENCES

[1] X. Gu and B. Zhu, ''Detection and correction of cycle slip in triple-frequency GNSS positioning,'' *IEEE Access*, vol. 5, pp. 12584–12595, 2017.
[2] Y. Zhao, ''Applying time-differenced carrier phase in nondifferential GPS/IMU tightly coupled navigation systems to improve the positioning performance,'' *IEEE Trans. Veh. Technol.*, vol. 66, no. 2, pp. 992–1003, Feb. 2017.
[3] G. Stienne, S. Reboul, M. Azmani, J. B. Choquel, and M. Benjelloun, ''GNSS dataless signal tracking with a delay semi-open loop and a phase open loop,'' *Signal Process.*, vol. 93, no. 5, pp. 1192–1209, May 2013.
[4] Y. Li, M. Wu, X. Du, T. Song, and P. Kam, ''A refinement to the Viterbi-Viterbi carrier phase estimator and an extension to the case with a Wiener carrier phase process,'' *IEEE Access*, vol. 7, pp. 78170–78184, 2019.
[5] A. Razavi, D. Gebre-Egziabher, and D. M. Akos, ''Carrier loop architectures for tracking weak GPS signals,'' *IEEE Trans. Aerosp. Electron. Syst.*, vol. 44, no. 2, pp. 697–710, Apr. 2008.
[6] J. Yin, R. Tiwari, and M. Johnston, ''Robust GPS carrier tracking model using unscented Kalman filter for a dynamic vehicular communication channel,'' *IEEE Access*, vol. 6, pp. 26930–26938, 2018.
[7] F. Fohlmeister, A. Iliopoulos, M. Sgammini, F. Antreich, and J. A. Nossek, ''Dual polarization beamforming algorithm for multipath mitigation in GNSS,'' *Signal Process.*, vol. 138, pp. 86–97, Sep. 2017.
[8] B. Qiu, W. Liu, and R. B. Wu, ''Blind interference suppression for satellite navigation signals based on antenna arrays,'' in *Proc. IEEE China Summit Int. Conf. Signal Inf. Process. (ChinaSIP)*, Beijing, China, Jul. 2013, pp. 370–373.
[9] D. Zhang, J. Zhang, C. Cui, W. Wu, and D. Fang, ''Single RF channel digital beamforming array antenna based on compressed sensing for large-scale antenna applications,'' *IEEE Access*, vol. 6, pp. 4340–4351, 2018.
[10] Y. Schechtman, Y. C. Eldar, O. Cohen, H. N. Chapman, J. Miao, and M. Segev, ''Phase retrieval with application to optical imaging: A contemporary overview,'' *IEEE Signal Process. Mag.*, vol. 32, no. 3, pp. 87–109, Mar. 2015.
[11] T. Gerkmann, M. Krawczyk-Becker, and J. L. Roux, ''Phase processing for single-channel speech enhancement: History and recent advances,'' *IEEE Signal Process. Mag.*, vol. 32, no. 2, pp. 55–66, Mar. 2015.
[12] A. S. Bandeira, J. Cahill, D. G. Mixon, and A. A. Nelson, ''Saving phase: Injectivity and stability for phase retrieval,'' *Appl. Comput. Harmon. Anal.*, vol. 37, no. 1, pp. 106–125, Jul. 2014.
[13] P. Netrapalli, P. Jain, and S. Sanghavi, ''Phase retrieval using alternating minimization,'' *IEEE Trans. Signal Process.*, vol. 63, no. 18, pp. 4814–4826, Sep. 2015.
[14] R. W. Gerchberg, ''A practical algorithm for the determination of phase from image and diffraction plane pictures,'' *Optik*, vol. 35, no. 2, pp. 237–246, 1972.
[15] E. J. Candès, T. Strohmer, and V. Voroninski, ''Phaselift: Exact and stable signal recovery frommagnitude measurements via convex programming,'' *Commun. Pure Appl. Math.*, vol. 66, no. 8, pp. 1241–1274, Aug. 2013.
[16] E. J. Candès, X. Li, and M. Soltanolkotabi, ''Phase retrieval via wirtinger flow: Theory and algorithms,'' *IEEE Trans. Inf. Theory*, vol. 61, no. 4, pp. 1985–2007, Apr. 2015.
[17] T. Qiu, P. Babu, and D. P. Palomar, ''PRIME: Phase retrieval via majorization-minimization,'' *IEEE Trans. Signal Process.*, vol. 64, no. 19, pp. 5174–5186, Oct. 2016.
[18] G. Wang, G. B. Giannakis, and Y. Eldar, ''Solving random systems of quadratic equations via truncated amplitude flow,'' *IEEE Trans. Inf. Theory*, vol. 64, no. 2, pp. 773–794, Feb. 2018.
[19] G. Wang, L. Zhang, G. B. Giannakis, M. Akçakaya, and J. Chen, ''Sparse phase retrieval via truncated amplitude flow,'' *IEEE Trans. Signal Process.*, vol. 66, no. 2, pp. 479–491, Jan. 2018.
[20] T. Qiu and D. P. Palomar, ''Undersampled sparse phase retrieval via majorization-minimization,'' *IEEE Trans. Signal Process.*, vol. 65, no. 22, pp. 5957–5969, Nov. 2017.
[21] R. Varadhan and C. Roland, ''Simple and globally convergent methods for accelerating the convergence of any EM algorithm,'' *Scand. J. Statist. Theory Appl.*, vol. 35, no. 2, pp. 335–353, 2008.
[22] R. Salakhutdinov and S. Roweis, ''Adaptive over relaxed bound optimization methods,'' in *Proc. Int. Conf. Mach. Learn.*, 2003, pp. 664–671.
[23] A. Beck and M. Teboulle, ''A fast iterative shrinkage-thresholding algorithm for linear inverse problems,'' *SIAM J. Imag. Sci.*, vol. 2, no. 1, pp. 183–202, Mar. 2009.
[24] J. Song, P. Babu, and D. P. Palomar, ''Optimization methods for designing sequences with low autocorrelation sidelobes,'' *IEEE Trans. Signal Process.*, vol. 63, no. 15, pp. 3998–4009, Aug. 2015.
[25] J. T. Curran, G. Lachapelle, and C. C. Murphy, ''Digital GNSS PLL design conditioned on thermal and oscillator phase noise,'' *IEEE Trans. Aerosp. Electron. Syst.*, vol. 48, no. 1, pp. 180–196, Jan. 2012.
[26] S. A. Vorobyov, ''Principles of minimum variance robust adaptive beamforming design,'' *Signal Process.*, vol. 93, no. 12, pp. 3264–3277, Dec. 2013.
[27] J. B. Y. Tsui, *Fundamentals of Global Positioning System Receivers: A Software Approach*, 2nd ed. New York, NY, USA: Wiley, 2005.
[28] Y. L. Wang, H. Chen, and Y. N. Peng, *Theory and Algorithm of Spatial Spectrum Estimation*. Beijing, China: Tsinghua Univ. Press, 2004.
[29] S. Miller, X. Zhang, and A. Spanias, *Multipath Effects in GPS Receivers: A Primer*. San Rafael, CA, USA: Morgan & Claypool, 2015.
[30] G. Xie, *Principles of GPS and Receiver Design*. Beijing, China: House of Electronics Industry, 2009.
[31] K. Borre, D. M. Akos, N. Bertelsen, P. Rinder, and S. H. Jensen, *A Software-Defined GPS and Galileo Receiver*. Boston, MA, USA: Birkhäuser, 2007.

QIANG LI received the Ph.D. degree in navigation guidance and control from Harbin Engineering University, China, in 2015. From 2015 to 2018, he was a Postdoctoral Researcher with the College of Information Engineering, Shenzhen University. He joined the Communication Group, University of Sheffield, U.K., in 2016, as a Visiting Scholar, where he researched the phase retrieval algorithms for antenna array. He is currently an Associate Research Fellow with the College of Electronics and Information Engineering, Shenzhen University. His research interests include array signal processing, satellite navigation, and phase retrieval algorithms.

LEI HUANG (M'07–SM'14) received the B.Sc., M.Sc., and Ph.D. degrees in electronic engineering from Xidian University, Xi'an, China, in 2000, 2003, and 2005, respectively.

From 2005 to 2006, he was a Postdoctoral Fellow with the Department of Electrical and Computer Engineering, Duke University, Durham, NC, USA. He also held the Research Fellow and Research Associate positions at the City University of Hong Kong, Hong Kong, and The Chinese University of Hong Kong, Hong Kong. From 2012 to 2014, he was a Full Professor with the Department of Electronics and Information Engineering, Harbin Institute of Technology (Shenzhen), Xili, Shenzhen. Since November 2014, he has been with the College of Electronics and Information Engineering, Shenzhen University, as a Distinguished Professor, and established the Shenzhen Key Laboratory of Advanced Navigation Technology (ANT) as the Founding Director. He is currently the Vice Dean of the College of Electronics and Information Engineering, Shenzhen University. His research interests include spectral estimation, array signal processing, statistical signal processing, and their applications in radar, navigation and wireless communications. In these areas, he has published 75 IEEE journal articles, and has undertaken 20 national and provincial key projects, such as the Key Project of NSFC and Joint Project of NSFC-RGC (Hong Kong).

Dr. Huang was the winner of the Distinguished Young Scientists of NSFC, Program of New Century Excellent Talents in University of Ministry of Education (MOE) of China, and a Leading Talent of Special Support Program of Guangdong Province. He won the second prize of the Natural Science Award in University of MOE of China, in 2015. He was an Associate Editor of IEEE TRANSACTIONS ON SIGNAL PROCESSING (2015–2019), and has been severing as a Senior Area Editor of this journal, since April 2019. He has also been on the editorial boards of the *Digital Signal Processing* (Elsevier) (2012–present) and the *IET Signal Processing* (2017–present), and an elected member of the Sensor Array and Multichannel (SAM) Technical Committee of the IEEE Signal Processing Society (2016–present). He was elected an IET Fellow, in 2018, and a Distinguished Young Scholar in China.

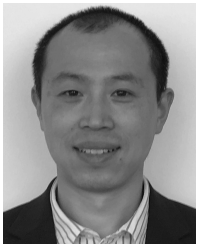

WEI LIU (S'01–M'04–SM'10) received the B.Sc. and LLB degrees from Peking University, China, in 1996 and 1997, respectively, the M.Phil. degree from The University of Hong Kong, in 2001, and the Ph.D. degree from the School of Electronics and Computer Science, University of Southampton, U.K., in 2003.

He then held a postdoctoral position first at Southampton and later at the Department of Electrical and Electronic Engineering, Imperial College London. Since September 2005, he has been with the Department of Electronic and Electrical Engineering, University of Sheffield, U.K., first as a Lecturer and then a Senior Lecturer. He has published about 300 journal and conference papers, five book chapters, and two research monographs titled "*Wideband Beamforming: Concepts and Techniques*" (John Wiley, March 2010) and the "*Low-Cost Smart Antennas*" (Wiley-IEEE, March 2019), respectively. His research interests include a wide range of topics in signal processing, with a focus on sensor array signal processing and its various applications, such as robotics and autonomous systems, human–computer interface, radar, sonar, satellite navigation, and wireless communications. He is an elected member of the Digital Signal Processing Technical Committee of the IEEE Circuits and Systems Society and the Sensor Array and Multichannel Signal Processing Technical Committee of the IEEE Signal Processing Society (Vice-Chair from Jan 2019). He was an Associate Editor for the IEEE TRANSACTIONS ON SIGNAL PROCESSING (March 2015–March 2019) and is currently an Associate Editor for IEEE ACCESS, and an editorial board member of the *Journal Frontiers of Information Technology and Electronic Engineering*.

BO ZHAO (M'15) was born in Henan, China, in 1986. He received the B.Sc. and Ph.D. degrees from Xidian University, Xi'an, China, in 2010 and 2015, respectively. From 2015 to 2018, he was a Postdoctoral Researcher with the College of Information Engineering, Shenzhen University. He is currently an Assistant Professor with the College of Information Engineering, Shenzhen University. His research interests include radar imaging, SAR countermeasure, and compressive sensing.

PEICHANG ZHANG received the B.Eng. degree (Hons.) in electronic engineering from the University of Central Lancashire, Preston, U.K., in 2009, and the M.Sc. and Ph.D. degrees in wireless communications from the University of Southampton, Southampton, U.K., in 2010 and 2015, respectively. He is currently with the College of Information and Engineering, Shenzhen University, China. His research interests include antenna selection, coherent and non-coherent detection, iterative detection, as well as channel estimation.